Proceedings of the
Third European Conference on Structural Control, 3ECSC,
12-15 July 2004, Vienna University of Technology, Vienna, Austria

DYNAMICS OF PHASE BOUNDARIES IN THERMOELASTIC SOLIDS

Arkadi Berezovski [1], Jüri Engelbrecht [2], Gérard A. Maugin [3]

[1,2] *Centre for Nonlinear Studies, Institute of Cybernetics at Tallinn University of Technology, Akadeemia tee 21, 12618, Tallinn, Estonia*
[3] *Laboratoire de Modélisation en Mécanique, Université Pierre et Marie Curie, UMR 607, Tour 66, 4 Place Jussieu, Case 162, 75252, Paris Cédex 05, France*

The high damping capacity of the thermoelastic martensitic phase is related to the hysteretic movement of interfaces. The modeling of moving phase boundaries in the context of the continuum description of stress-induced martensitic phase transformations in solids is a complicated problem. Phase-transition front propagation in solids is a non-linear process even if states of a solid before and after phase transformation are described by linear thermoelasticity theory. Numerical simulation of the phase-transition front propagation deals not only with the solution of conservation laws of mass, linear momentum, and energy, but also with the jump relations at the phase boundary. The equilibrium jump relations are definitely invalid after the initiation of the phase transformation because of a fast propagation of sharp phase interfaces through the material. In this paper, results of numerical simulations of phase-transition front propagation in solids are presented based on non-equilibrium thermodynamic conditions at the phase boundary.

Keywords: *martensitic phase transformations, dynamic loading, moving phase boundaries, damping*

1 Introduction

Shape memory alloys attract increasing interest as materials that can be used for damping applications. The passive high damping capacity of SMA is related to the hysteretic movement of different phase interfaces (Ref [1]). Civil engineering applications of SMA are recently attracting more attention, especially for protection of civil constructions against earthquake vibration damage (Ref. [2], [3]). With reference to seismic vibrations, design of constructions relies on the capability of structural elements of dissipating energy, so as to survive a severe earthquake without collapse.

The austenitic phase is stable before the application of a stress, but at some critical stress the martensite becomes stable, causing a stress plateau. Since the martensite is only stable because of the applied stress, the austenite structure again becomes stable during unloading, and the original undeformed shape is recovered. The unloading occurs at a lower stress level due to transformational hysteresis. When the stress is released, the martensite transforms back into austenite and the specimen returns to its original shape. The superelastic behavior is based on the movement of phase boundaries during the martensitic phase transformation.

At the same time, the modeling of moving phase boundaries in the context of the continuum description of stress-induced martensitic phase transformations in solids is a complicated problem. Phase-transition front propagation in solids is a non-linear process even if states of a solid before and after phase transformation are described in the framework of linear thermoelasticity theory. Numerical simulation of the phase-transition front propagation deals not only with the solution of equations expressing the conservation laws of mass, linear momentum, and energy, but also with the jump relations at the phase boundary. The system of jump relations is not closed. The extensive study of the problem shows that the velocity of a moving phase boundary cannot be determined in the framework of continuum mechanics without any additional hypotheses. As it is well known, the phase transformation begins only after some critical values of parameters are reached. The lack of the constitutive information follows from equilibrium jump relations at the phase boundary. The equilibrium conditions are definitely invalid after the initiation of the phase

[1] Dr, arkadi.berezovski@cs.ioc.ee
[2] Professor, je@ioc.ee
[3] Professor, gam@ccr.jussieu.fr

transformation because of a fast propagation of sharp phase interfaces through the material. In this paper, non-equilibrium thermodynamic conditions at the phase boundary (Ref. [4]) are used to describe the propagation of phase-transition fronts in crystalline solids. As a consequence, a thermodynamically consistent form of the finite-volume numerical method for the simulation of phase-transition front propagation is obtained (Ref. [5]). The results of simulations are compared with the experimental data for the impact-induced martensitic phase transformation. This comparison shows that the developed model simulations capture the experimentally observed stress-strain relations.

2 Uniaxial motion of a slab

Following Ref. [6], we consider the simplest possible formulation of the problem, namely, the uniaxial motion of a slab. Consider a slab, which in an unstressed reference configuration occupies the region $0 < x < L,\ -\infty < y, z < \infty,$ and consider uniaxial motion of the form

$$v_i = v_i(x,t), \sigma_{ij} = \sigma_{ij}(x,t), \tag{1}$$

for velocity and stress fields v_i and σ_{ij}. In this case, we have only three non-vanishing components of the strain tensor. Without loss in generality, we can set third component equal to zero due to zero initial and boundary conditions for this component and obtain uncoupled systems of equations for longitudinal and shear components. We focus attention on the system of equations for shear components, because the martensitic phase transformation is expected to be induced by shear.

2.1 Dynamic problem

We seek piecewise smooth velocity and stress fields $v(x,t),\ \sigma(x,t)$ in inhomogeneous thermoelastic materials subject to the following initial and boundary conditions:

$$\sigma(x,0) = v(x,0) = 0, \tag{2}$$

$$v(0,t) = v_0,\ \sigma(l,t) = 0, \tag{3}$$

where v_0 is given constant.

The unknown fields obey the field equations:

$$\frac{\partial}{\partial t}\left(\rho(x)\, v\right) = \frac{\partial \sigma}{\partial x}, \tag{4}$$

$$\frac{\partial}{\partial t}\left(\frac{\sigma}{\mu(x)}\right) = \frac{\partial v}{\partial x}, \tag{5}$$

where ρ is the density and μ is shear modulus.

2.2 Phase boundary kinetics

To consider the possible irreversible transformation of a phase into another one, the separation between the two phases is idealized as a sharp, discontinuity surface ***S*** across which most of the fields suffer finite discontinuity jumps.

Let $[A]$ and $\langle A \rangle$ denote the jump and mean value of a discontinuous field A across ***S***, the unit normal to ***S*** being oriented from the ``minus'' to the ``plus'' side:

$$[A] = A^+ - A^-, \quad \langle A \rangle = (A^+ + A^-)/2 \tag{6}$$

.

The phase transition fronts considered are homothermal (no jump in temperature; the two phases coexist at the same temperature) and coherent (they present no defects such as dislocations). Consequently, we have the following continuity conditions in terms of temperature, T, and material velocity, V, (Ref. [7]):

$$[T] = 0,\ [V] = 0\,. \tag{7}$$

The jump relations associated with the balance of linear momentum and balance of entropy read (Ref. [7])

$$V_N[\rho v] + [\sigma] = 0, \tag{8}$$

$$V_N[S] - \left[\frac{k}{T}\frac{\partial T}{\partial x}\right] = \sigma_s \geq 0, \tag{9}$$

where S is entropy, V_N is the normal component of the material velocity of the points of ***S***, and σ_S is the entropy production at the interface.

As shown in Ref. [7], the entropy production can be expressed in terms of the driving force f_S such that the dissipation at the interface reads

$$f_s\, V_N = T_s \sigma_s \geq 0, \tag{10}$$

where T_S is the temperature at ***S***.

The driving force at the interface between phases is found in the form (Ref. [7]):

$$f_s = -[\sigma\varepsilon] + 2\langle\sigma\rangle[\varepsilon]\ . \tag{11}$$

3 Algorithm description

The system of Eqs (4)-(5) is solved numerically by means of a finite-volume numerical scheme

$$v_n^{k+1} = v_n^k - \frac{\Delta t}{\rho_n \Delta x}\left((\Sigma^+)_n^k - (\Sigma^-)_n^k\right), \tag{12}$$

$$v_n^{k+1} = v_n^k - \mu_n \frac{\Delta t}{\Delta x}\left((V^+)_n^k - (V^-)_n^k)\right), \tag{13}$$

where the contact quantities $\Sigma^{\pm}$ and $V^{\pm}$ are determined at any interface between adjacent elements without phase transformation as follows:

$$\left(\Sigma^+\right)_{n-1}^k - \left(\Sigma^-\right)_n^k = \left(\sigma\right)_n^k - \left(\sigma\right)_n^k \quad , \tag{14}$$

$$\left(V^+\right)_{n-1}^k - \left(V^-\right)_n^k = \left(v\right)_n^k - \left(v\right)_{n-1}^k \quad . \tag{15}$$

If the value of the driving force at the phase boundary exceeds the critical one (Ref. [5])

$$f_{\text{critical}} = -\frac{T_0^2}{2}\left[\alpha(3\lambda+2\mu)\right]\left\langle\frac{\alpha(3\lambda+2\mu)}{\lambda+2\mu}\right\rangle, \tag{16}$$

we apply another set of rules at the phase boundary:

$$\left(\Sigma^+\right)_{n-1}^k - \left(\Sigma^-\right)_n^k = 0\,, \tag{17}$$

$$\left(V^+\right)_{n-1}^k - \left(V^-\right)_n^k = 0. \tag{18}$$

The direction of the front propagation is determined by the positivity of the entropy production (Eq. (10)). The material velocity at the interface is determined by means of the jump relation for linear momentum (Eq. (8)).

4 Numerical results

The geometry of the problem is shown in Fig. 1. The wave is excited at the left boundary of the computation domain by prescribing a time variation of the shear component of the stress tensor. Upper and bottom boundaries are stress-free, the right boundary is assumed to be rigid.

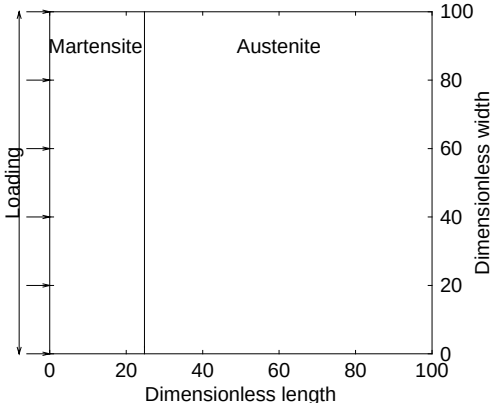

Figure 1: Geometry of the problem.

If the magnitude of the wave is high enough, the phase transformation process is activated at the phase boundary. The maximal value of the Gaussian pulse is chosen as 0.7 GPa. Material properties correspond to Cu-14.44Al-4.19Ni shape-memory alloy (Ref. [8]): in austenitic phase the density is 7100 kg/m^3, the elastic modulus E = 120 GPa, the shear wave velocity c_s = 1187 m/s, the dilatation coefficient is 6.7510 10^{-6} 1/K. It was recently reported (Ref. [9]) that elastic properties of martensitic phase after impact loading are very sensitive to the amplitude of loading. Therefore, for the martensitic phase we choose, respectively, E = 60 GPa, c_s = 1055 m/s, with the same density and dilatation coefficient as above. As a first result of computations, the stress-strain relation is plotted in Fig. 2 at a fixed point inside the computational domain which was initially in the austenitic state.

The stress-strain relation is at first linear corresponding to elastic austenite. Then the strain value jumps along a constant stress line to its value in the martensitic state due to the phase transformation. The value of the strain jump between straight lines, the slope of which is prescribed by material properties of austenite and martensite, respectively, is determined by the value of stress that conforms to the critical value of the driving force. This critical value of the driving force is also determined by the material properties (see Eq. (16)). The critical value of the driving force should agree with the barrier of potential that we have to overcome to go from one phase to the other. Therefore, the stress value corresponding to the critical value of the driving force can be associated with the transformation stress, and the value of the strain jump is nothing else but the transformation strain.

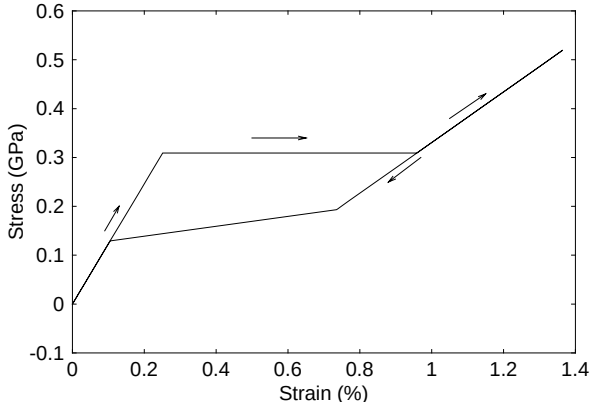

Figure 2: Local stress-strain behavior at a fixed point with full recovering of austenite.

If value of reference temperature is above the onset of reverse transformation temperature, we should expect that the austenitic state will be recovered after unloading. The inverse phase transformation should occur immediately when the actual deformation of martensitic elements become less than the

transformation strain. Since the inverse transformation is governed by another condition than the direct transformation, we obtain a hysteretic stress-strain behavior (Fig. 2). The overall stress-strain dependence is compared with experimental data. Corresponding results are shown in Fig. 3, where the experimental data of a quasi-static loading with relatively high applied loading rate (1 MPA/s) from Ref. [10] are given.

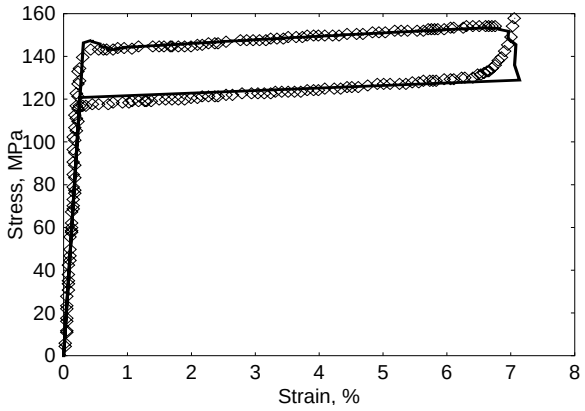

Figure 3: Stress-strain relation at the phase boundary: comparison with experimental data from Ref. [10]. Solid line corresponds to the numerical simulation.

The obtained stress-strain behavior results in a specific interaction between a plane stress wave and the phase boundary. The result of the interaction is shown in Fig. 4 that represents the structure of the interaction of the incoming wave (from left) with the phase boundary. We observe here that amplitudes of both transmitted and reflected waves are cut off, whereas the phase boundary has moved into the austenitic region from its initial position. Therefore, the martensitic phase transformation exhibits a property to be a filter for the amplitudes of incoming waves. The magnitude of the transmitted wave in Fig. 4 corresponds to the value of the transformation stress.

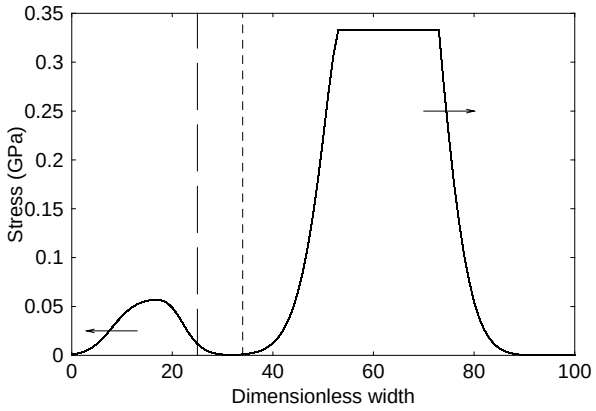

Figure 4: Plane wave profile after interaction with moving phase boundary. Dashed line corresponds to initial position of the phase boundary, dotted line – to the final one.

Acknowledgments

Support of the Estonian Science Foundation under contracts No. 4504, 5765 (A.B., J.E.) and of the European Network TMR. 98-0229 on "Phase transitions in crystalline substances" (G.A.M.) is gratefully acknowledged. G.A.M. benefits from a Max Planck Award for International Cooperation (2001-2005). Research carried on within the Parrot French-Estonian Program (2003-2004).

References

[1] Van Humbeeck, J., Damping Capacity of Thermoelastic Martensite in Shape Memory Alloys. *Journal of Alloys and Compounds,* Vol. 355, p.58, 2003.

[2] Mazzolani, F.M. and Mandara, A., Modern Trends in The Use of Special Metals for the Improvement of Historical and Monumental Structures. *Engineering Structures*, Vol. 24, p.843, 2002.

[3] Desroches, R. and Smith, B., Shape Memory Alloys in Seismic Resistant Design and Retrofit: A Critical Review of their Potential and Limitations. *Journal of Earthquake Engineering,* Vol. 8, p. 415, 2004.

[4] Berezovski, A. and Maugin, G.A., On the Thermodynamic Conditions at Moving Phase-Transition Fronts in Thermoelastic Solids. *Journal of Non-Equilibrium Thermodynamics,* Vol. 29, p.37, 2004.

[5] Berezovski, A. and Maugin, G.A., Thermoelastic Wave and Front Propagation. *Journal of Thermal Stresses,* Vol. 25, p.719, 2002.

[6] Abeyaratne, R., Bhattacharya, K. and Knowles, J.K., Strain-Energy Functions with Local Minima: Modeling Phase Transformations Using Finite Thermoelasticity. In: Fu, Y., Ogden, R.W., (Eds.), *Nonlinear Elasticity: Theory and Application*. Cambridge University Press, pp. 433-490, 2001.

[7] Maugin, G.A., On Shock Waves and Phase-Transition Fronts in Continua. *ARI, Vol.* 50, p.141, 1998.

[8] Escobar, J.C. and Clifton, R.J., On Pressure-Shear Plate Impact for Studying the Kinetics of Stress-Induced Phase-Transformations. *Material Science and Engineering, Vol.* A170, p.125, 1993.

[9] Emel'yanov, Y., et al. Detection of Shock-Wave-Induced Internal Stresses in Cu-Al-Ni Shape Memory Alloy by Means of Acoustic Technique. *Scripta Materialia,* Vol. 43, p.1051, 2000.

[10] Goo, B.C. and Lexcellent, C., Micromechnics-Based Modeling of Two-Way Memory Effect of a Single-Crystalline Shape-Memory Alloy. *Acta Materialia,* Vol. 45, p.727, 1997.